Front. Earth Sci. 2016, 10(2): 303–314
DOI 10.1007/s11707-016-0545-8

RESEARCH ARTICLE

Mapping rice cropping systems using Landsat-derived Renormalized Index of Normalized Difference Vegetation Index (RNDVI) in the Poyang Lake Region, China

Peng LI[1,2], Luguang JIANG[1], Zhiming FENG (✉)[1], Sage SHELDON[3], Xiangming XIAO[3]

1 Institute of Geographic Sciences and Natural Resources Research, Chinese Academy of Sciences, Beijing 100101, China
2 Key Laboratory of Poyang Lake Wetland and Watershed Research, Ministry of Education, Jiangxi Normal University, Nanchang 330022, China
3 Department of Botany and Microbiology, Center for Spatial Analysis, University of Oklahoma, Norman, OK 73019, USA

Abstract Mapping rice cropping systems with optical imagery in multiple cropping regions is challenging due to cloud contamination and data availability; development of a phenology-based algorithm with a reduced data demand is essential. In this study, the Landsat-derived Renormalized Index of Normalized Difference Vegetation Index (RNDVI) was proposed based on two temporal windows in which the NDVI values of single and early (or late) rice display inverse changes, and then applied to discriminate rice cropping systems. The Poyang Lake Region (PLR), characterized by a typical cropping system of single cropping rice (SCR, or single rice) and double cropping rice (DCR, including early rice and late rice), was selected as a testing area. The results showed that NDVI data derived from Landsat time-series at eight to sixteen days captures the temporal development of paddy rice. There are two key phenological stages during the overlapping growth period in which the NDVI values of SCR and DCR change inversely, namely the ripening phase of early rice and the growing phase of single rice as well as the ripening stage of single rice and the growing stage of late rice. NDVI derived from scenes in two temporal windows, specifically early August and early October, was used to construct the RNDVI for discriminating rice cropping systems in the polder area of the PLR, China. Comparison with ground truth data indicates high classification accuracy. The RNDVI approach highlights the inverse variations of NDVI values due to the difference of rice growth between two temporal windows. This makes the discrimination of rice cropping systems straightforward as it only needs to distinguish whether the candidate rice type is in the period of growth ($RNDVI < 0$) or senescence ($RNDVI > 0$).

Keywords Normalized Difference Vegetation Index (NDVI), Renormalized Index of NDVI (RNDVI), rice cropping systems, phenology, temporal windows, Poyang Lake Region (PLR)

Received February 17, 2015; accepted June 18, 2015

E-mail: fengzm@igsnrr.ac.cn

1 Introduction

Paddy rice is one of the three most important crops in China, accounting for nearly 35% of the total sown area of cereal crops in 2010 (National Bureau of Statistics of China, 2010). Over 95% of the rice area is located in southern China, the Middle-lower Yangtze River Plain, the Sichuan Basin, and northern China (Xiong et al., 2009). As China is undergoing rapid land use changes due to urbanization, a large amount of farmland has recently been transformed (Chen, 2007), and favorable agricultural policies have heavily impacted household-based rice cropping patterns (Li et al., 2012). Information on the distribution of paddy rice cultivation is essential for field management and yield estimation (Thenkabail, 2003), optimal water resource utilization (Bouman and Tuong, 2001), and greenhouse gas emission monitoring (Li et al., 2005).

Remote sensing has been used to discriminate rice cropping systems for decades; and the launch of the Moderate Resolution Imaging Spectroradiometer (MODIS) instrument in 1999 spurred a considerable number of publications (Xiao et al., 2005; Sakamoto et al., 2006; Xiao et al., 2006; Sakamoto et al., 2009a). Time-series of MODIS vegetation/water indices (e.g., Normalized Difference Vegetation Index, NDVI; Enhanced

Vegetation Index, EVI; and Land Surface Water Index, LSWI) are commonly utilized in rice cropping systems classification and hold considerable potential for large-scale monitoring (Xiao et al., 2005, 2006). However, a major issue for temporal profiles of vegetation indices derived from satellite images with moderate to coarse spatial resolution is the mixed-pixel effect that prevents accuracy (Sakamoto et al., 2005, 2009b; Xiao et al., 2005, 2006; Wardlow et al., 2007; Peng et al., 2011). This may well explain why most to-date MODIS time-series analysis has been conducted primarily in northern China, predominantly large flat plains with simple cropping patterns (Zhang et al., 2008). In southern China, cultivated land plots are small and fragmentized, and the pattern of cropping systems is complex (double to triple annually). The agricultural management practice founded in household units tends to change rice planting patterns year by year. Therefore, time-series analysis of MODIS and other sensors of coarse spatial resolution to classify cropping patterns are limited in this region. Synthetic aperture radar (SAR) data (e.g., European Remote Sensing Satellite and ENVISAT) can also be utilized in regional rice cropping systems delineation, and has great potential in subtropical and tropical areas due to its all-weather observation capability, as in the Mekong River Delta (Liew et al., 1998; Bouvet et al., 2009). However, the cost and inaccessibility of SAR data limits extensive investigations.

Another important optical data option is Landsat imagery. The historical images have been underutilized in mapping multi-year cropping patterns (Bastiaanssen et al., 2000; Martínez-Casasnovas et al., 2005). Indeed, Landsat Thematic Mapper (TM) and Enhanced Thematic Mapper plus (ETM+) data cannot meet the demand of finer spatial and temporal resolution simultaneously, and, moreover, overcast and rainy weather during the summer season in southern China usually yields only a few cloud-free Landsat images for a given region per year. Accordingly, only a few studies on rice cropping systems monitoring with Landsat imagery are reported. In these studies however, scientists combined certain images acquired during critical temporal windows showing distinct and unique spectral features with a local crop calendar to monitor cropping patterns (Van Niel and McVicar, 2004; Gusso and Ducati, 2012). It is expected that the freely available historical multi-decadal Landsat data will provide more data opportunities to carry out crops growth monitoring (Hansen and Loveland, 2012).

Rice cropping systems range from single- to triple-cultivation each year along the latitudinal gradient from north to south in China. Multiple rice cropping systems mapping in southern China is more complex than mono-culture rice system mapping in northern China. In a previous study, a single-date Landsat image was used to discriminate single- and double-cropping rice in the Poyang Lake Region (PLR) with a threshold method (Li et al., 2012). Landsat time-series analysis alone, however, cannot discriminate rice cropping systems due to the limit of imagery availability. In this paper, a phenology-based algorithm, the Renormalized Landsat-derived NDVI (RNDVI) was proposed based on two temporal windows in which the NDVI values of single and early (or late) rice changed inversely, and was then applied to map rice cropping systems in the PLR. The objective of this study is twofold: (i) to assess the potential of the RNDVI approach derived from Landsat imagery in discriminating rice cropping systems at the regional scale; and (ii) to compare the performance of the RNDVI and threshold methods. If feasible, the RNDVI approach can be applicable in other regions with double to triple rice cropping systems.

2 Materials and methods

2.1 Study area

Located in northern Jiangxi Province and the central Yangtze River Basin, Poyang Lake is the largest freshwater lake in China. It collects water from five major rivers (the Ganjiang, Fuhe, Xinjiang, Raohe, and Xiushui) in Jiangxi Province, and then flows into the Yangtze River through the outlet in Hukou County (Fig. 1). Throughout the year, the natural water surface area of Poyang Lake changes tremendously due to the fluctuations of water level, varying from approximately 3,500 km^2 in the summer season to about 600 km^2 in the winter season (Li, 2012). This unique hydrological phenomenon profoundly effects agricultural production in the PLR. The PLR is one of the major rice production areas in China and covers twelve counties or districts around the lake (Fig. 1) with a total paddy field area of 6,147 km^2 (Li et al., 2012). According to the Jiangxi Statistical Yearbook from 2002 to 2010 (http://chinadataonline.org/), the sown area of rice accounts for more than 90% of the total sown area of all crops and the output of rice makes up over 95% of the total output of grain in the PLR.

There are two characteristic rice planting systems in the PLR each year, namely double cropping rice (DCR) and single cropping rice (SCR). DCR consists of early rice and late rice that are sequentially cultivated in the same paddy field. It generally begins with sowing in late March, and harvest in mid-late July for early rice, and then late rice seedlings transplantation in late July (sometimes in early August) and harvest in late October. SCR is often called single rice (or middle rice) locally. Sowing begins in late May, and harvesting ends in early October. Many factors may influence farmers' preferences of rice cropping practices year by year, including agriculture policies, market price, labor force, and irrigation conditions. In a previous study we found that the favorable agriculture policies enacted since 2004 have directly motivated farmers to plant more DCR in this region (Li et al., 2012).

For any given paddy field, the cultivation of SCR and

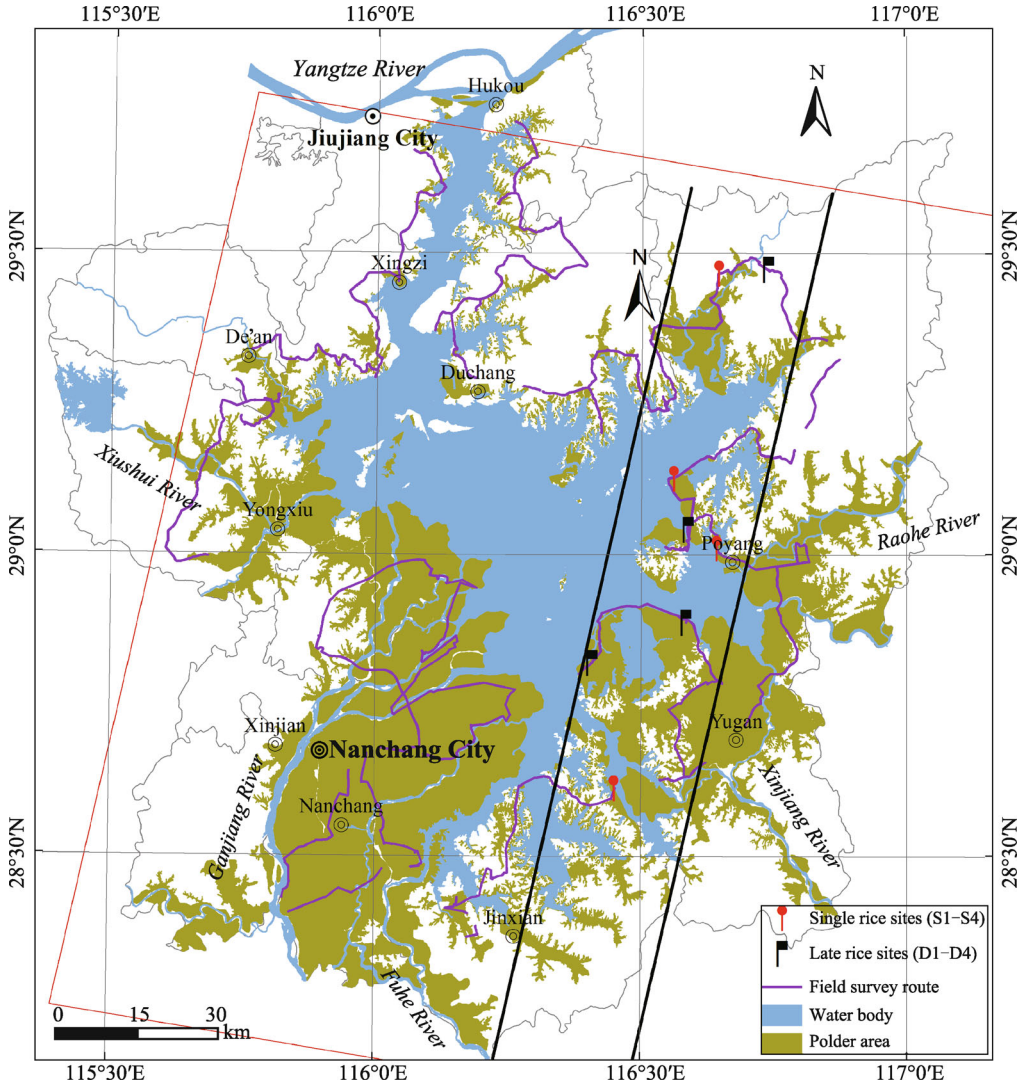

Fig. 1 Location of the study area showing the distribution of the Poyang Lake and polder area in the PLR. Note that the area between the two parallel black solid lines is the middle part of Landsat-7 ETM+ scene (path/row, 121/40), approximately 22 kilometers wide. This area is also known as Scan Line Corrector (SLC) on image without data gaps.

DCR is spatially independent. The calendar of annual rice growing systems in the PLR (Fig. 2) was established with a time interval of ten days according to the agro-meteorological datasets (Li et al., 2012). However, the actual rice calendar may be advanced or postponed for a few days due to meteorological factors like flood and drought. The temporal development of paddy fields can be characterized by three main periods: 1) the land preparation, flooding, and seedlings transplantation period; 2) the growing period (vegetative, reproductive, and ripening phases); and 3) the fallow period after harvest (Le Toan et al., 1997). According to the International Rice Research Institute, the vegetative phase starts at germination, continues through seedling, transplanting, tillering, and ends at stem elongation. The reproductive phase begins at panicle initiation and heading, and ends at flowering. The ripening phase covers the milk grain, dough grain, and maturity grain stages.

In the past, land reclamation via levee building has been the major way to increase farmland from lake area (Shankman and Liang, 2003). The levee system protects about 55% of fertile rice fields from floods in the PLR (Li, 2012) (Fig. 1). The polder area is mainly distributed along the lake and river delta areas with an elevation of less than 30 m. Paddy fields in the polder area are generally flat and concentrated. A levee map of Poyang Lake (Fig. 1) was visually interpreted and digitalized based on the *Levee Atlas of Jiangxi Province* (Jiangxi Province Department of Water Resources, 1999), field surveys, and one ETM+ scene (Table 1). In this paper, the polder area in the PLR was used as an experimental area to test the potential for rice cropping systems discrimination with the RNDVI.

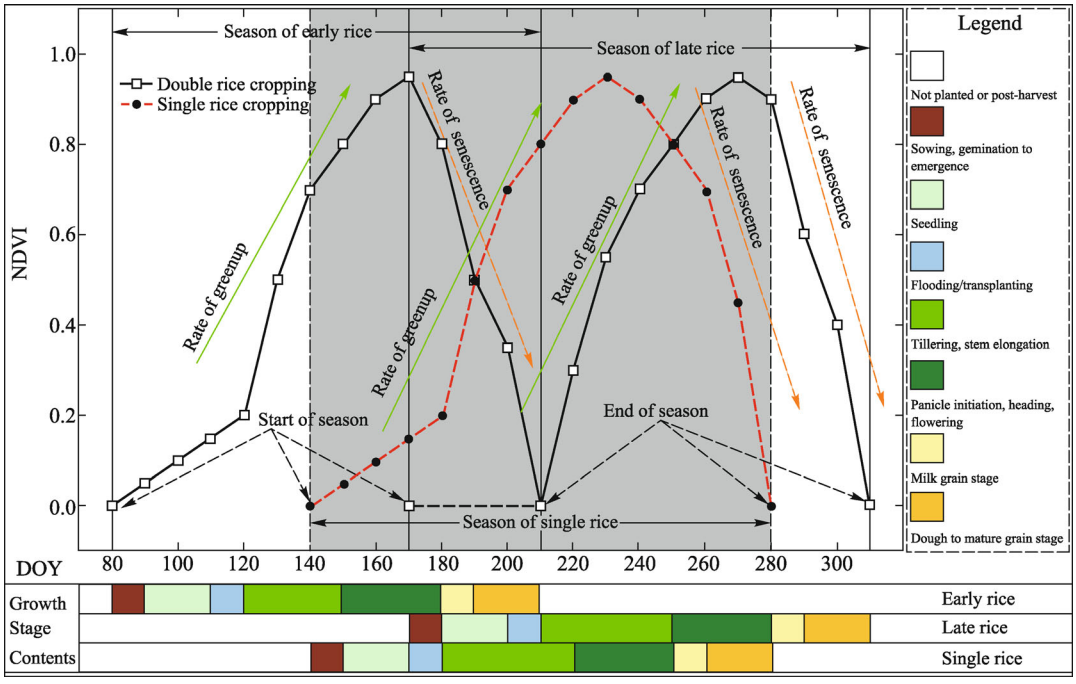

Fig. 2 Rice growth calendar at ten-day intervals in the PLR. There is a time interleaving between early- and late-rice from late June to late July. That is because local farmers normally leave several rice fields which are about ten percent of the total area of double cropping rice annually for raising seedlings of late rice. Late rice will be transplanted right after the harvesting of early rice, with the time difference less than three days. (DOY, day of year).

2.2 Landsat images and pre-processing

Three Landsat path/row scenes cover the polder area of the PLR: 121/40, 121/39, and 122/40. Multi-temporal TM/ETM+ images (30 m, 18 scenes in total, see Table 1) from 2010 were acquired. Among them, three TM images (No. 4, No. 8, and No. 14 in Table 1) were gathered from the Center for Earth Observation and Digital Earth (CEODE), Chinese Academy of Sciences (CAS) (http://ids.ceode.ac.cn/), and the other 15 scenes were available from the Global Visualization Viewer (GloVis) of USGS (http://glovis.usgs.gov/). Image to image registrations for the three TM scenes were conducted with the Root Mean Square Error (RMS error) to less than a half pixel (15 m). Images obtained from USGS GloVis are standard level-one terrain-corrected (L1T) products. They have undergone systematic radiometric and geometric corrections and overall geometric fidelity with ground control points and a digital elevation model ensured (NASA Goddard Space Flight Center, 2011). In 2003, the Scan Line Corrector (SLC) mechanism on-board Landsat 7 permanently failed. Therefore, for the ETM+ SLC-off images used for rice cropping systems classification, multi-image adaptive local regression proposed by the International Scientific Data Service Platform, Computer Network Information Center, CAS (http://datamirror.csdb.cn) was applied to fill in gaps to improve data usability. This method generally used 1−2 images (same path/row) acquired during a similar time frame in adjacent years.

Cloud contamination is another issue during the rice growing season, obscuring paddy fields and leading to underestimation of the corresponding NDVI. All cloud contaminated observation sites were excluded from further analysis. Furthermore, each Landsat image (121/40) was atmospherically corrected using the Fast Line-of-sight Atmospheric Analysis of Spectral Hypercubes (FLAASH) algorithm (Adler-Golden et al., 1999) in the Environment for Visualizing Images (ENVI, Version 4.7) software to obtain surface reflectance for NDVI calculation. FLAASH incorporates the Moderate Resolution Transmission (MODTRAN) 4 radiative transfer code. In this study, model parameters describing the mid-latitude summer- and winter-atmosphere and rural aerosols together with 2-band (K−T) aerosols retrieval were utilized in FLAASH.

NDVI is a useful indicator of plant growth condition (Tucker, 1979), and is calculated as a normalized ratio between Red and Near-infrared (NIR) bands:

$$\mathrm{NDVI} = (\rho_{\mathrm{NIR}} - \rho_{\mathrm{Red}})/(\rho_{\mathrm{NIR}} + \rho_{\mathrm{Red}}), \qquad (1)$$

where ρ_{NIR} and ρ_{Red} stand for the surface reflectance measurements of NIR and Red bands, respectively, which in turn correspond to the fourth and third bands of Landsat TM/ETM+ images. The values of NDVI range from minus one (−1.0) to plus one (+ 1.0), and negative

Table 1 List of Landsat TM/ETM+ images of 2010 used in this study. Note that No. 13 and No. 14 refer to the scenes of P/R 121/39 and 122/40 and other 16 time-series scenes are from 121/40

No.	Date	Cloud cover/%	Sensor	Usage	No.	Date	Cloud cover/%	Sensor	Usage
1	01/14/2010	0	TM	a	10	08/18/2010	3	ETM+	a, d
2	02/23/2010	0	ETM+	a	11	09/19/2010	5	ETM+	a, d
3	03/11/2010	0	ETM+	a	12	10/05/2010	0	ETM+	a, b, c, d, e
4	03/19/2010	0	TM	a	13	10/05/2010	0	ETM+	b, c
5	04/28/2010	13	ETM+	a	14	10/04/2010	0	TM	b, c
6	05/30/2010	34	ETM+	a, d	15	10/21/2010	39	ETM+	a, d
7	06/15/2010	43	ETM+	a, d	16	11/06/2010	0	ETM+	a
8	07/25/2010	1.3	TM	a	17	11/22/2010	24	ETM+	a
9	08/02/2010	3	ETM+	a, d, e	18	12/08/2010	0	ETM+	a

In the column of "Usage", a = calculating NDVI; b = interpreting the levee map in the PLR; c = interpreting paddy field map in the PLR; d = choosing training samples for single- and double-cropping rice fields; e = developing the RNDVI algorithm.

values typically correspond to open water and positive values (over 0.05) represent the amount of green vegetation present (Myneni et al., 1997).

2.3 Establishment of Renormalized Index of NDVI (RNDVI)

Beginning on September 18, 2010, an 8-day ground survey of different rice cropping systems (late rice and single rice) was conducted across the PLR (Fig. 1). Handheld global positioning system (GPS) receivers (Trimble Juno-SB) were used to collect each site's geographical location information (latitude, longitude, and elevation). 148 GPS points of rice field were recorded: 57 for single rice and 91 for late rice. To ensure the validity of these GPS points, all of the observed paddy sites were located within cropland-dominated areas. The linear distance between any two GPS points was at least 1.0 km. However, about 15%−25% of the GPS records coincided with SLC-off gaps for each ETM+ scene. The gaps are noticeable along the edge of each scene and gradually diminish towards the scene center. Furthermore, the precise locations of the missing scan areas vary from scene to scene. It therefore is impossible to construct temporal profiles of NDVI with those GPS points. That said, eight sample points (four for single rice and late rice each) located in the gap-free region were used to delineate the temporal dynamics of rice growth at the field level (Fig. 1).

NDVI values of DCR exhibited a bimodal distribution, while those of SCR displayed a unimodal distribution (Fig. 3). During the rice growth periods, high NDVI values were approximately 0.80−0.90 in the panicle initiation to heading stage, while low NDVI values were around 0−0.20 during the flooding/transplanting stage. Before the sowing of early rice (February to early March), paddy fields were primarily covered by shallow water or exposed soils. The corresponding NDVI values were generally below 0.40 and occasionally negative due to waterlogging in the rice fields. This phenomenon is more common for SCR than DCR. In fact, the waterlogging issue is one reason for cultivating a single rice crop per year. After transplanting, the NDVI values increase rapidly and then reach a plateau during the period of panicle initiation to heading. As rice plants develop into the ripening phase, i.e., milk, dough, yellow-ripe, and mature stages, their leaves gradually turn from green to a yellowish golden color due to a decrease in chlorophyll pigmentation. Correspondingly, NDVI values decline during the rice ripening stage and then drop significantly just after harvesting. The post-harvest paddy fields were mainly composed of residual rice plants and exposed soils. The corresponding NDVI values generally varied from 0.20−0.40.

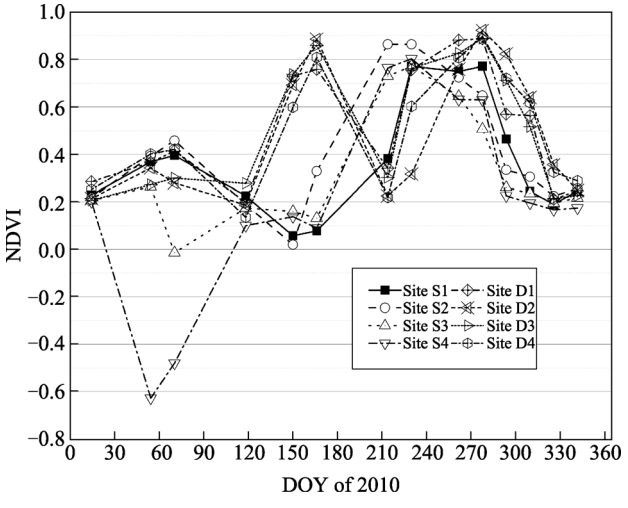

Fig. 3 Temporal dynamics of NDVI curves constructed with typical paddy fields sampling sites in the PLR. Note that the negative NDVI values imply the corresponding paddy fields which were caused by waterlogging from January to early March.

Land cover of rice fields for any given rice type (early, single, and late rice) cycle through shallow water (0.10−

0.15 m depth), growing rice plants, and exposed soils phases during the entire growth period. Generally, there is one high value (for growing rice plants) and two low values (for shallow water or exposed soils) in the NDVI curve for each season of paddy rice (Li et al., 2012). Temporal profiles of NDVI differ significantly between rice cropping systems during a given temporal window. Based on the NDVI variations of different cropping rice, several time windows were determined (Li et al., 2012). The RNDVI was created using the principle similar to that of the NDVI equation with two NDVI values of SCR and DCR (early rice or late rice) within two temporal windows in which the NDVIs showed inverse changes. The formula of the RNDVI is defined as follows:

$$\mathrm{RNDVI}=(|\mathrm{NDVI}_{t1}|-|\mathrm{NDVI}_{t2}|)/(|\mathrm{NDVI}_{t1}|+|\mathrm{NDVI}_{t2}|), \quad (2)$$

where $t1$ and $t2$ refer to the acquisition date of each scene in which the derivative NDVI values of single rice (field) and early or late rice (field) should change inversely. NDVI_{t1} and NDVI_{t2} are the NDVI values calculated from two Landsat images acquired during two different temporal windows with Eq. (1). Similarly, the value range of the RNDVI varies from −1.0 to +1.0. Negative RNDVI values indicate that the NDVIs of the candidate rice type increased from $t1$ to $t2$, thus identifying a growing period while positive RNDVI values show that the NDVIs of the other candidate rice type decreased from $t1$ to $t2$, i.e., a senescencing period.

It is important to note that NDVI temporal dynamics of SCR and DCR show noticeable differences from May to October, an overlapping growth period. As displayed in Fig. 3, the high NDVI values of early, single, and late rice appear in June, August, and September, respectively, while the low values of corresponding rice types appear in late April to early May, late June to early July, and late July to early August, respectively. From the perspective of individual rice plants' growth process, they all undergo a growth period as the NDVI values increase from zero to peak values, and a senescence period as the NDVI values decrease to low values. It is interesting to note that NDVI values of SCR and DCR show exactly the opposite trend between early June and October. Therefore, for early/late rice and single rice, it was easy to find two critical temporal windows with corresponding opposite values of NDVIs for the RNDVI calculation.

2.4 Classification of rice cropping systems with RNDVI

In subtropical regions, it is difficult to collect good-quality time-series Landsat images due to cloud coverage. Two major approaches were distinguished based on whether single-date or multi-temporal images would be used. As single rice and early (or late) rice have a time interval of over a month (Fig. 2), there are two temporal windows in which the NDVI values of the two types of rice are inverses of each other. The first window is the period when early rice is in its senescencing stage while single rice is just in the growing stage. The second is the period when single rice is in the senescencing stage while late rice is in the growing stage. Thus, the RNDVI was proposed to discriminate SCR and DCR based on whether the candidate rice type is in a stage of growth ($\mathrm{RNDVI}<0$) or senescence ($\mathrm{RNDVI}>0$) between two observations. In this paper, time-series temporal profiles of NDVI at the field level served as indicators for describing the physical properties of the paddy rice system. A paddy rice calendar was used to select temporal windows for constructing the RNDVI according to acquired Landsat images. The paddy field map served as a mask to avoid interference from other land cover types. Two images (acquired on August 2 and October 5, 2010) were utilized to calculate the RNDVI for the rice cropping map (Fig. 4).

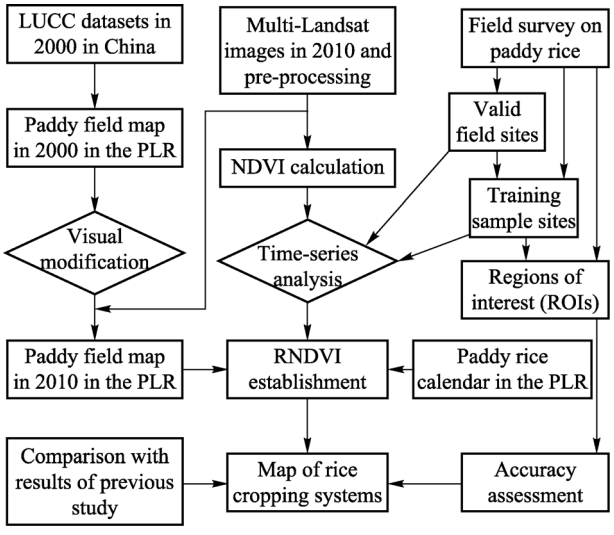

Fig. 4 The flowchart for mapping rice cropping system using the RNDVI derived from Landsat images in the PLR.

A paddy field distribution map from 2010 was used as a base map for rice cropping systems classification. The base map was visually interpreted with three cloud-free Landsat TM/ETM+ images (Table 1) and updated based on the paddy field map of the 2000 National Land Cover Dataset developed by the Chinese Academy of Sciences. The paddy field map of 2000 was also interpreted from Landsat imagery with a validated accuracy over 90% (Liu et al., 2005). Since the polder area in the PLR is flat and low (less than 30 m above sea level), visual interpretation ensured a high accuracy (over 95%) of rice paddy distribution.

2.5 Accuracy assessment and comparison

The accuracy assessment of classification results for SCR and DCR identified using the RNDVI approach was

evaluated with ground truth points of paddy rice collected in 2010 and regions of interest (ROI) of single- and late-rice generated based on phenological rice features. A unique physical feature of paddy fields is that the corresponding land-cover cycles through exposed soils, shallow water, and rice plants annually. Remotely sensed observations captured these phenological and physiological changes. Based on this physical feature, 225 ROI polygons (37,923 pixels) were generated to carry out accuracy assessments using a confusion matrix. These polygons were chosen from seven ETM+ images (Table 1) and followed three basic rules. First, the ROI polygons were distributed in farmland. Second, they were not affected by cloud or cloud shadow and SLC failure. Third, and most importantly, the ROIs of single rice fields are covered by shallow water or exposed soils or a mixture for two images (acquired on May 30 and June 15, 2010), and covered by rice plants for the other two images (August 2 and August 18, 2010). For those of double rice, fields are covered by shallow water or exposed soils or a mixture for one image (August 2), and covered by rice plants for the other five images (May 30, June 15, September 19, October 5, and October 21).

In addition, in a previous study, a threshold method of NDVI derived from one single-date image acquired on October 5 was used to delineate rice cropping systems in the PLR in 2010. This study highlighted the phenological and physiological differences between single rice and late rice in a critical temporal window (Fig. 2). However, subjective threshold determination tends to affect classification results. Besides, much work will be done to determine the thresholds when this approach introduced to other areas. The RNDVI approach proposed in this study is also a phenology-based algorithm that focuses on the phenological and physiological changes in different rice cropping systems within two time windows. The RNDVI approach is viewed as a developed version of the threshold method. In this paper, we also compared the performance of the two methods.

3 Results

3.1 Mapping rice cropping systems and accuracy assessment

Theoretically, any two time windows with reversed NDVI values for single rice and early (or late) rice would be suitable for the RNDVI formula. For example, we could use the images on June 15 and August 2 (or 18), 2010 to calculate the RNDVI to differentiate early rice from single rice and utilize the images on August 2 (or 18) and October 5 (or September 19), 2010 to compute the RNDVI to distinguish single rice from late rice. However, the images (June 15, August 18, and September 19, 2010) are partially cloud-contaminated. The image on October 21, 2010 also cannot be used for RNDVI computation because some late rice plants were in the harvesting stage during late October. In this study, NDVI data from the two Landsat ETM+ images (path/row, 121/40) taken on August 2 and October 5, 2010, were used to establish the RNDVI. From early August to early October, late rice plants grow rapidly from green-up after the transplanting stage to the milk grain stage with increased NDVI values, while single rice plants undergo a transition from the stem elongation stage to post-harvest stage with decreased NDVI values. The positive RNDVI values represented single rice, or SCR, whereas the negative RNDVI values stood for late rice, viz. DCR. The paddy field area in the polder area of the PLR was about 3,366 km^2, of which 99.5% was covered by one scene (path/row, 121/40). We used just the polder area of the PLR covered by the 121/40 scene as the experimental area. The classification results showed that the area of SCR and DCR were 508 km^2 and 2,842 km^2, respectively. Figures 5(a) displays the spatial pattern of SCR and DCR in the polder area of the PLR in 2010. Spatially, DCR was the dominant planting pattern, while SCR was mainly located in the lower reach of Xiushui River.

There were 69 observation sites for late rice and only six observation sites for single rice located in the polder area. The classification accuracies of late rice and single rice were 97% and 83%, respectively. The accuracy assessment for DCR is encouraging. However, that of SCR may not be convincing due to the limited GPS sampling sites in the polder area. Meanwhile, the resultant maps of SCR and DCR were assessed using a confusion matrix based on ROIs (37,923 pixels) for validation (Table 2). The overall accuracy was 98.9% with the Kappa coefficient of 0.976. Besides, accuracy assessment was conducted for the classification results derived from the threshold method with the same ground truth data (Table 3), and its results showed that the RNDVI approach performed much better than the threshold method in discriminating rice cropping systems.

3.2 Comparison with the classification results derived from threshold method

In our previous study, a single-date Landsat scene was used to discriminate SCR and DCR with a threshold method. This method may be subjective when determining the threshold values. The RNDVI approach, which uses two dates to capture phenological and physiological change information, is a more developed version of the threshold method that only uses single date. The results of this study were compared with that derived from the threshold method in our previous study (Li et al., 2012) at the farm and landscape scales. According to the fieldwork, the green areas within the peony pink ellipse in Fig. 6(a) and the sage green to gray areas within the peony pink ellipse in

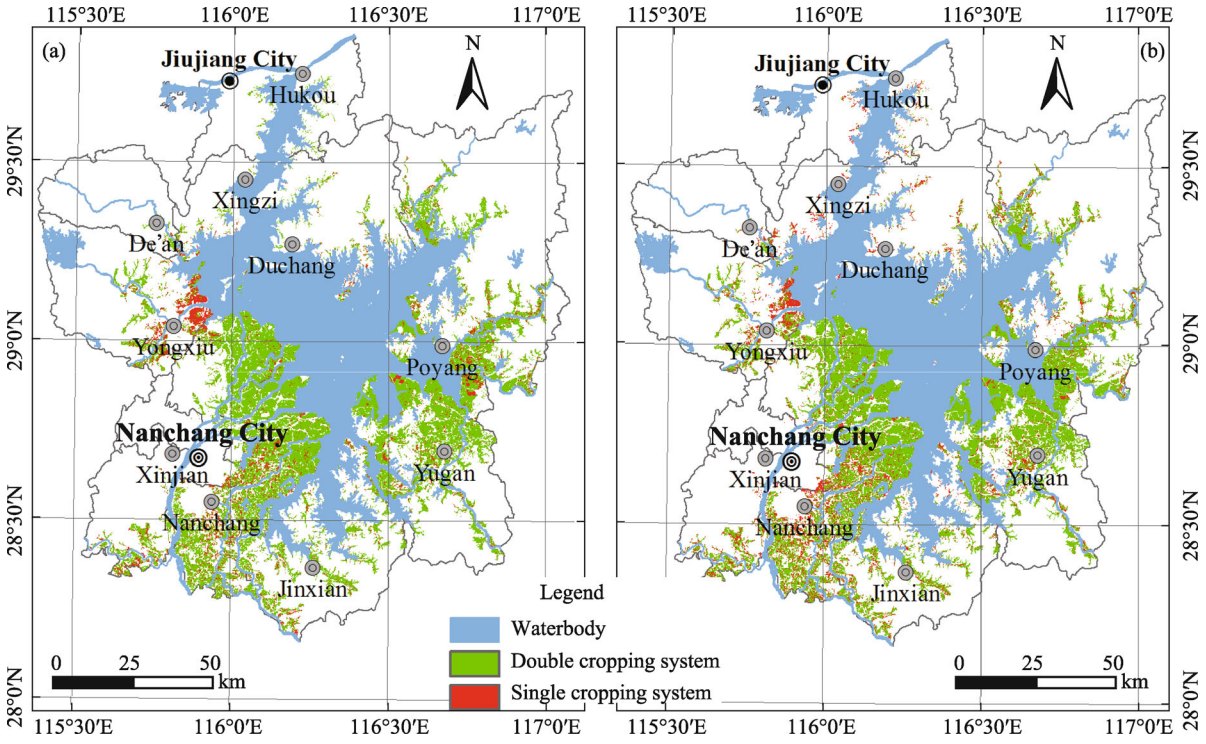

Fig. 5 Spatial pattern of different rice cropping systems derived from the RNDVI approach (a) and threshold method (b) with Landsat-7 ETM+ images in 2010 in the polder area of the PLR. The water bodies in blue color were extracted from the Landsat-7 ETM+ scene acquired on October 5, 2010.

Table 2 Accuracy assessment of the classification map of SCR and DCR based on the RNDVI approach in this study

Class		Ground truth samples (pixels)		Total classified pixels	Producer accuracy
		Single rice	Double rice		
Classified results	Single rice	13,505	425	13,930	96.9%
	Double rice	0	23,993	23,993	100%
Total ground truth pixel		13,505	24,418	37,923	
User accuracy		100%	98.3%		

Overall accuracy is 98.9%; Kappa coefficient is 0.976.

Table 3 Accuracy assessment of the classification map of SCR and DCR based on the threshold method in a previous study

Class		Ground truth samples (pixels)		Total classified pixels	Producer accuracy
		Single rice	Double rice		
Classified results	Single rice	7,937	5,993	13,930	57.0%
	Double rice	0	23,993	23,993	100%
Total ground truth pixel		7,937	29,986	37,923	
User accuracy		100%	80.0%		

Overall accuracy is 84.2%; Kappa coefficient is 0.697.

Fig. 6(b) were all single rice fields in 2010. However, the results obtained from the RNDVI (Fig. 6(c)) were closer to the actual situation than those from the threshold method (Fig. 6(d)). At the landscape scale, the classification results Fig. 5(b) were derived from one ETM+ image (path/row 121/40, October 5, 2010) with the threshold method. The major reason for using this single scene to distinguish SCR from DCR was the obvious difference in growth stages. It was taken in the period of harvesting or post-harvest for single rice and the milk grain stage for late rice. Therefore, paddy fields with an NDVI between 0.55 and 1.0 were classified as DCR, while paddy fields with positive NDVI

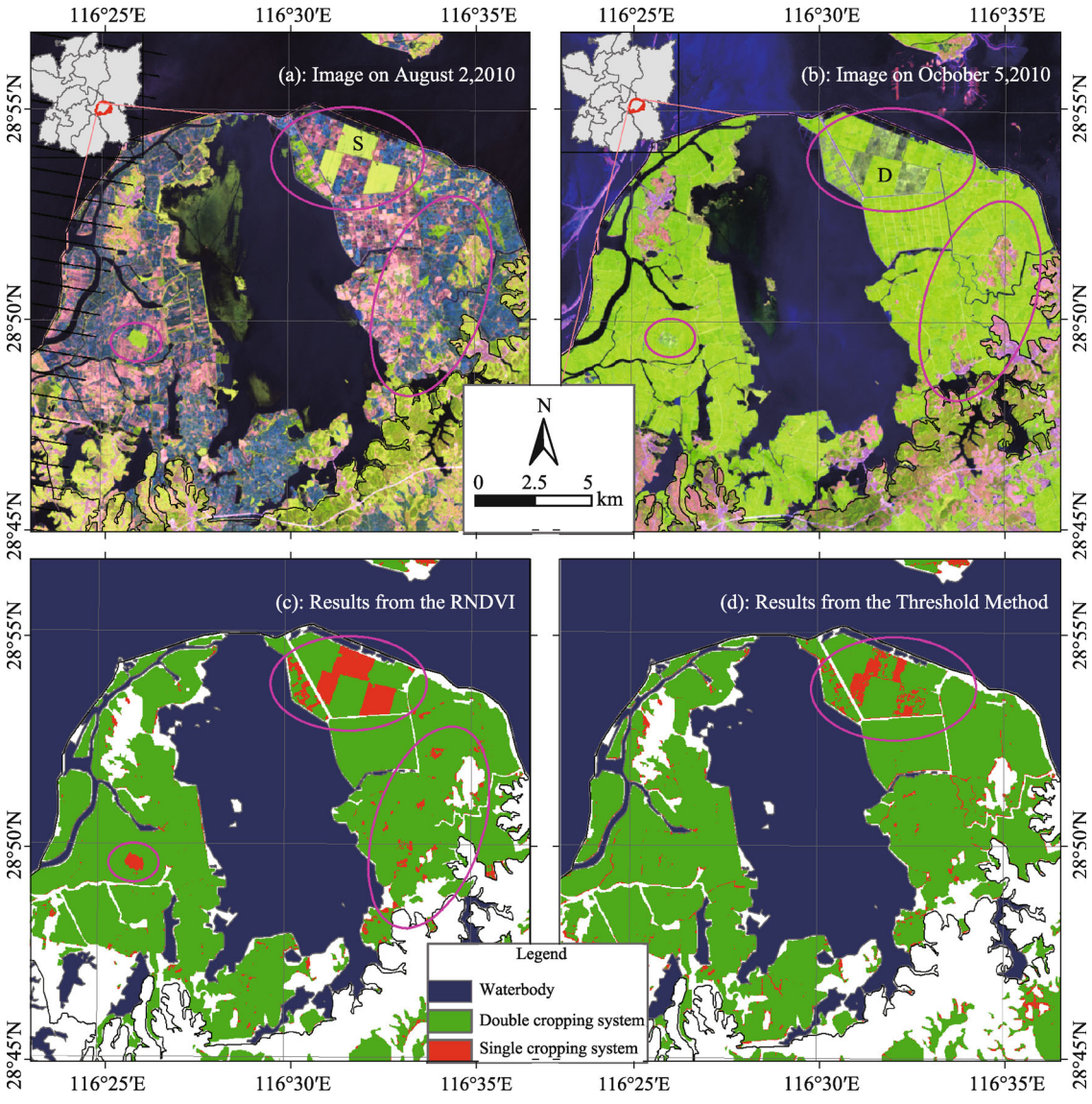

Fig. 6 Difference of paddy rice (fields) imaging in the Kangshan Flood Storage Diversion Area in Yugan County during two temporal windows in 2010. Note that the capital letter S refers to single cropping rice, while D stands for double cropping rice. Figure 6(a): single rice is in the panicle initiation to heading stage and late rice is in the transplanting stage. Figure 6(b): single rice is in the harvesting or post-harvest stage and late rice is in the filling/milking stage. Figures 6(c) and 6(d) refer to the classification results obtained from the RNDVI approach and threshold method, respectively.

less than 0.54 were classified as SCR. Correspondingly, the areas of SCR and DCR were 726 km^2 and 2,611 km^2, respectively. Compared with the results derived from the RNDVI, the area of SCR was overestimated while the area of DCR was underestimated.

4 Discussion

In this study, a phenology-based algorithm, the Renormalized Index of NDVI (RNDVI) was proposed and applied to map rice cropping systems by using temporal change in NDVI based on rice phenology. In 2010, the PLR was predominately cultivated by DCR, implying a very high intensity of rice planting for a traditional single and double rice cropping area. This can be illustrated by the multiple-cropping index (MCI), which is the ratio of total area with planted and harvested crops to the total cultivated area per year. The MCI is an important indicator for measuring cropping intensity (Panigrahy et al., 2011). The rice cropping index, however, was already up to 184.8% in the polder area of the PLR in 2010, and the potential of enhancing rice production in the polder area of the PLR by increasing the MCI is limited.

Compared with the threshold method, which involves subjective judgements in determining thresholds, the

RNDVI approach performs better in discriminating rice cropping systems. Rice production is household-based in this study area, and farmers have to sow or transplant rice within a given period. Nevertheless, the time gap of sowing or transplanting for various paddies always exists. For example, there are nearly 7-day variations between the southern counties (e.g., Nanchang and Xinjian) and the northern county (Hukou) or district (i.e., Lushan), and from the west to the east of the PLR, as well. Even in the same county or district there may be about three days of difference for a given growth stage. Year-to-year temporal differences in rice planting in a certain locality may also reach several days. These differences will be much larger for the vast area of the middle and lower reaches of Yangtze River Basin. It is therefore quite challenging to determine threshold values. For a certain available image during the growing season, the growth stages of early, single, or late rice may not be completely identical. This may yield discrepancies in NDVI within rice cropping systems. For example, the NDVI of any given late rice field entering into mature grain stage may be less than 0.55 and thus may be falsely classified as single rice. By contrast, the RNDVI approach highlights temporal change in NDVI caused by rice's phenological patterns, from land preparation, flooding for transplanting, tillering, heading to harvesting. The RNDVI approach has clear scientific merit and objectivity. For any two temporal windows, if SCR (or DCR, e.g., early rice or late rice) is in the growing period while the DCR (or single rice) is in the senescencing period, the RNDVI approach can be used.

Three factors could affect rice cropping systems mapping when using the RNDVI method within critical temporal windows. The first factor is the limited data availability due to the impact of frequent cloud cover in the subtropical area. This problem is universal in the usage of optical satellite data. However, in July and August of each year, the PLR, as well as the middle and lower reaches of Yangtze River Basin, are often under the control of the subtropical high pressure belt, which usually leads to hot and dry weather. During September and October, the region typically has little precipitation. This allows the acquisition of cloud free or little cloud coverage images from June to October. According to USGS GloVis and CEODE, there are 45 TM, ETM+, and Landsat-8 Operational Land Imager (OLI) scenes (path/row = 121/40) with little cloud coverage (less than 10%) from 2009 to 2013. Among them, 23 scenes were acquired in June–October, 17 scenes in November–March, and five scenes in April and May.

The second factor is the data loss (22%) of ETM+ images due to the SLC-off failure since 2003. What is worse, the precise locations of the missing scan lines vary from scene to scene. Though there are some reports on gap-filling methods, these methods can not completely restore data to the original level, as they primarily utilize existing images such as SLC-on and Landsat 5 to fill the gap. Therefore, classification errors in rice cropping systems mapping may be caused by filling the scan gap with inaccurate data. Also, the Landsat 7 ETM+ SLC-off problem may make some *in situ* field survey information invalid. For example, 15%–25% of total field sampling sites collected in this study during mid-late September were located in the SLC-off area of each image. One should take the SLC-off issue into consideration prior to conducting field surveys to avoid fruitless labor. However, the currently optional Landsat-8 also provides routine image acquisition that can avoid the SLC-off problem.

Finally, as paddy fields are small and usually mixed with other land cover types in southern China, the mixed pixel problem may be a challenge to rice cropping systems mapping. The use of the paddy map as a mask may greatly reduce misclassification, as the area of rice fields (over 0.1 ha) is generally larger than one pixel of Landsat image (0.09 ha). Finer spatial resolution imagery for the land-use interpretation (especially for rice paddies) will significantly improve the reliability of intra-rice cropping systems classification.

In subtropical and tropical Asia, where rice fields are widely distributed (Thenkabail et al., 2005), using MODIS-derived vegetation indices to map paddy rice leads to underestimation of the area of paddy fields due to the small patch size (Xiao et al., 2005, 2006). This study further proves that finer spatial resolution images would provide more information on the regional cropping pattern (Martínez-Casasnovas et al., 2005; Chen et al., 2011). The RNDVI derived from Landsat imagery during critical temporal windows could greatly reduce the data requirements for mapping cropping patterns compared with the time series method. Therefore, this approach will be of great practical use in other double rice cropping areas, e.g., the middle and lower Yangtze River Basin and triple rice cropping regions like southern China and mainland Southeast Asia.

5 Conclusions

Multiple rice cropping systems are widely practiced in tropical and subtropical regions to enhance grain production. However, accurate mapping of multiple cropping systems is very important but usually difficult when using optical remote sensing data due to weather conditions, temporal and spatial resolutions, and data availability. Two main approaches are generally categorized depending on the utilization of single-date or time-series images. Single-date discrimination is usually doubted due to the subjectivity in determining the appropriate thresholds. Time-series analysis with Landsat imagery is often heavily restricted by data availability. In this study, a phenology-based algorithm, the Renormalized Index of NDVI (RNDVI), was proposed and applied to discriminate rice cropping systems in the Poyang Lake Region. Although

multiple images from 2010 were used to delineate the temporal development of NDVI of different rice cropping systems, the RNDVI was developed based on only two temporal windows in which the NDVI values of SCR and DCR displayed inverse change. The two time windows refer to two distinct phenological phases: the senescencing stage of early rice (DCR) and the growing stage of single rice, and the senescencing stage of single rice and the growing stage of late rice (DCR). Two dates (scenes) which display different phenological information for single- and late-rice were used to calculate the RNDVI for mapping rice cropping systems in the polder area of the PLR in southern China. Comparison with ground truth data showed a high accuracy of 97% for late rice and 83% for single rice. In addition, the confusion matrix that was based on the random selection of validation pixels yielded an overall classification accuracy of 98.9% and Kappa coefficient of 0.976. The RNDVI approach performed much better than the threshold method in discriminating rice cropping systems. This study demonstrated that Landsat imagery from critical temporal windows hold the potential for discriminating rice cropping systems at a regional scale.

Acknowledgements This work was supported by the Key Program of the National Natural Science Foundation of China (Grant No. 41430861) and the Open Fund of Key Laboratory of Poyang Lake Wetland and Watershed Research, Ministry of Education, Jiangxi Normal University (PK2014010). We thank the U.S. Geological Survey (USGS) and the Center for Earth Observation and Digital Earth (CEODE) for providing Landsat TM/ETM+ data, and the Meteorological Information Center of China Meteorological Administration for providing agro-meteorological datasets. The critical comments of Professor Fang Hongliang from the Institute of Geographic Sciences and Natural Resources Research, and Senior Researcher Leon Braat from Wageningen University, helped to improve this manuscript. Thanks also go to Ms. Sarah Xiao from Yale University for her thoughtful English editing. We thank the anonymous reviewers for their insightful comments on earlier versions of the manuscript.

References

Adler-Golden S M, Matthew M W, Bernstein L S, Levine R Y, Berk A, Richtsmeier S C, Acharya P K, Anderson G P, Felde G, Gardner J, Hoke M L, Jeong L S, Pukall B, Ratkowski A J, Burke H K (1999). Atmospheric correction for short-wave spectral imagery based on MODTRAN 4. Proc. SPIE 3753, Imaging Spectrometry V, 61: 61–69

Bastiaanssen W G M, Molden D J, Makin I W (2000). Remote sensing for irrigated agriculture: examples from research and possible applications. Agric Water Manage, 46(2): 137–155

Bouman B, Tuong T P (2001). Field water management to save water and increase its productivity in irrigated lowland rice. Agric Water Manage, 49(1): 11–30

Bouvet A, Le Toan T, Lam-Dao N (2009). Monitoring of the rice cropping system in the Mekong delta using ENVISAT/ASAR dual polarization data. IEEE Transactions on Geoscience and Remote Sensing, 47(2): 517–526

Chen J (2007). Rapid urbanization in China: a real challenge to soil protection and food security. Catena, 69(1): 1–15

Chen J, Huang J, Hu J (2011). Mapping rice planting areas in southern China using the China Environment Satellite data. Math Comput Model, 54(3−4): 1037–1043

Gusso A, Ducati J R (2012). Algorithm for soybean classification using medium resolution satellite images. Remote Sens, 4(10): 3127–3142

Hansen M C, Loveland T R (2012). A review of large area monitoring of land cover change using Landsat data. Remote Sens Environ, 122 (Landsat Legacy Special Issue): 66–74

Jiangxi Province Department of Water Resources (1999). Levee Atlas of Jiangxi Province. Nanchang: Jiangxi Province Department of Water Resources

Le Toan T, Ribbes F, Wang L F, Floury N, Ding K H, Kong J A, Fujita M, Kurosu T (1997). Rice crop mapping and monitoring using ERS-1 data based on experiment and modeling results. IEEE Transactions on Geoscience and Remote Sensing, 35(1): 41–56

Li C S, Frolking S, Xiao X M, Moore B, Boles S, Qiu J J, Huang Y, Salas W, Sass R (2005). Modeling impacts of farming management alternatives on CO_2, CH_4, and N_2O emissions: a case study for water management of rice agriculture of China. Global Biogeochem Cy, 19 (GB30103): B3010, 10–1029

Li P (2012). Trade-off between Grain Production and Flood Regulation Functions in the Poyang Lake Region, China. Dissertation for Ph.D degree. Beijing: Institute of Geographic Sciences and Natural Resources Research, Chinese Academy of Sciences, 166

Li P, Feng Z, Jiang L, Liu Y, Xiao X (2012). Changes in rice cropping systems in the Poyang Lake Region, China during 2004−2010. J Geogr Sci, 22(4): 653–668

Liew S C, Kam S P, Tuong T P, Chen P, Minh V Q, Lim H (1998). Application of multitemporal ERS-2 synthetic aperture radar in delineating rice cropping systems in the Mekong River Delta, Vietnam. IEEE Transactions on Geoscience and Remote Sensing, 36(5): 1412–1420

Liu J Y, Liu M L, Tian H Q, Zhuang D F, Zhang Z X, Zhang W, Tang X M, Deng X Z (2005). Spatial and temporal patterns of China's cropland during 1990−2000: an analysis based on Landsat TM data. Remote Sens Environ, 98(4): 442–456

Martínez-Casasnovas J A, Martín-Montero A, Casterad M A (2005). Mapping multi-year cropping patterns in small irrigation districts from time-series analysis of Landsat TM images. Eur J Agron, 23(2): 159–169

Myneni R B, Keeling C D, Tucker C J, Asrar G, Nemani R R (1997). Increased plant growth in the northern high latitudes from 1981 to 1991. Nature, 386(6626): 698–702

NASA Goddard Space Flight Center (2011). Landsat 7 Science Data Users Handbook.http://landsathandbook.gsfc.nasa.gov/pdfs/Landsat7_Handbook.pdf

National Bureau of Statistics of China (2010). China Statistical Yearbook. Beijing: China Statistics Press

Panigrahy S, Ray S S, Manjunath K R, Pandey P S, Sharma S K, Sood A, Yadav M, Gupta P C, Kundu N, Parihar J S (2011). A spatial database of cropping system and its characteristics to aid climate change impact assessment studies. Journal of the Indian Society of Remote Sensing, 39(3): 355–364

Peng D, Huete A R, Huang J, Wang F, Sun H (2011). Detection and

estimation of mixed paddy rice cropping patterns with MODIS data. Int J Appl Earth Obs Geoinf, 13(1): 13–23

Sakamoto T, Van Cao P, Van Nguyen N, Kotera A, Yokozawa M (2009 a). Agro-ecological interpretation of rice cropping systems in flood-prone areas using MODIS imagery. Photogramm Eng Remote Sensing, 75(4): 413–424

Sakamoto T, Van Nguyen N, Ohno H, Ishitsuka N, Yokozawa M (2006). Spatio-temporal distribution of rice phenology and cropping systems in the Mekong Delta with special reference to the seasonal water flow of the Mekong and Bassac rivers. Remote Sens Environ, 100(1): 1–16

Sakamoto T, Van P C, Kotera A, Duy K N, Yokozawa M (2009b). Detection of yearly change in farming systems in the Vietnamese Mekong Delta from MODIS time-series imagery. Jarq-Jpn Agr Res Q, 43(3): 173–185

Sakamoto T, Yokozawa M, Toritani H, Shibayama M, Ishitsuka N, Ohno H (2005). A crop phenology detection method using time-series MODIS data. Remote Sens Environ, 96(3−4): 366–374

Shankman D, Liang Q L (2003). Landscape changes and increasing flood frequency in China's Poyang Lake Region. Prof Geogr, 55(4): 434–445

Thenkabail P S (2003). Biophysical and yield information for precision farming from near-real-time and historical Landsat TM images. Int J Remote Sens, 24(14): 2879–2904

Thenkabail P S, Schull M, Turral H (2005). Ganges and Indus river basin land use/land cover (LULC) and irrigated area mapping using continuous streams of MODIS data. Remote Sens Environ, 95(3): 317–341

Tucker C J (1979). Red and photographic infrared linear combinations for monitoring vegetation. Remote Sens Environ, 8(2): 127–150

Van Niel T G, McVicar T R (2004). Determining temporal windows for crop discrimination with remote sensing: a case study in south-eastern Australia. Comput Electron Agric, 45(1−3): 91–108

Wardlow B D, Egbert S L, Kastens J H (2007). Analysis of time-series MODIS 250 m vegetation index data for crop classification in the US Central Great Plains. Remote Sens Environ, 108(3): 290–310

Xiao X, Boles S, Frolking S, Li C, Babu J Y, Salas W, Moore B III (2006). Mapping paddy rice agriculture in South and Southeast Asia using multi-temporal MODIS images. Remote Sens Environ, 100(1): 95–113

Xiao X, Boles S, Liu J, Zhuang D, Frolking S, Li C, Salas W, Moore B III (2005). Mapping paddy rice agriculture in southern China using multi-temporal MODIS images. Remote Sens Environ, 95(4): 480–492

Xiong W, Conway D, Lin E D, Holman I (2009). Potential impacts of climate change and climate variability on China's rice yield and production. Clim Res, 40(1): 23–35

Zhang M W, Zhou Q B, Chen Z X, Liu J, Zhou Y, Cai C F (2008). Crop discrimination in Northern China with double cropping systems using Fourier analysis of time-series MODIS data. International Journal of Applied Earth Observation and Geoinformation, 10(4): 476–485